Chinese Chemical Letters 32 (2021) 565–568

Contents lists available at ScienceDirect

Chinese Chemical Letters

journal homepage: www.elsevier.com/locate/cclet

Communication

Synthesis and structure of $Au_{19}Ag_4(S\text{-}Adm)_{15}$ nanocluster: Polymorphs and optical properties

Xuemei Fu[a,b], Xinzhang Lin[a,b], Xiuqing Ren[a], Hengjiang Cong[c], Chao Liu[a,*], Jiahui Huang[a,*]

[a] Gold Catalysis Research Center, State Key Laboratory of Catalysis, Dalian Institute of Chemical Physics, Chinese Academy of Sciences, Dalian 116023, China
[b] University of Chinese Academy of Sciences, Beijing 100049, China
[c] College of Chemistry and Molecular Sciences, Engineering Research Center of Organosilicon Compounds & Materials, Ministry of Education, Wuhan University, Wuhan 430072, China

ARTICLE INFO

Article history:
Received 23 December 2019
Received in revised form 14 February 2020
Accepted 20 February 2020
Available online 21 February 2020

Keywords:
$Au_{19}Ag_4(S\text{-}Adm)_{15}$
Alloy nanocluster
Polymorph
Fluorescence
Thermal stability

ABSTRACT

Polymorphism is a common phenomenon in nature. Here, we report one-pot wet chemical method to synthesize two polymorphs of $Au_{19}Ag_4(S\text{-}Adm)_{15}$ nanocluster protected by 1-adamantanethiol (HS-Adm), which adopt P-1 and $P2_1/c$ space group respectively. The crystal structures of two polymorphs were determined by X-ray crystallography. Compared to the previously reported $Au_{19}Ag_4(S\text{-}Adm)_{15}$ nanocluster adopting $P2_1/n$ space group, polymorphs of $Au_{19}Ag_4(S\text{-}Adm)_{15}$ with P-1 and $P2_1/c$ space group show the different optical properties. Moreover, $Au_{19}Ag_4(S\text{-}Adm)_{15}$ with P-1 space group exhibits good thermal stability. Meanwhile, we investigated the effect of solvent and molar ratio of metal precursors on the polymorphs. This work provides an insight to polymorphs of metal nanoclusters.

Nobel metal nanoclusters have attracted significant attentions for decades in virtue of the potential applications in many fields, such as sensor [1–3], biochemistry [4–7], catalysis [8–11] and optics [12–14]. A series of atomically precise Au nanoclusters have been successfully synthesized and their crystal structures have been determined by X-ray crystallography. In recent years, most work concentrated on developing novel methods to design and synthesize special crystal structures of Au nanoclusters with enhanced properties. It has been found that Au-M alloy nanoclusters could exhibit synergistic effects on the physical and chemical properties due to the foreign atoms doping into Au nanoclusters [15,16]. Therefore, design, preparation and application in different fields of Au-M alloy nanoclusters have been a hot spot [17–23].

As doping foreign atoms can influence the electronic structure of Au nanoclusters, different metal atoms are brought into Au nanoclusters in order to tune the chemical and physical properties of Au nanoclusters. Fields-Zinna *et al.* successfully doped Pd into $Au_{25}(SR)_{18}$ nanocluster and obtained $PdAu_{24}(SR)_{18}$ alloy nanocluster *via* ligand exchange method [24]. After that, many foreign metal atoms, such as Ag [25–31], Pt [32,33], Cu [34–36], Hg [37,38] and Cd [37,38], were doped into thiolate protected Au nanoclusters. Wang *et al.* doped Cu, Ag, Cd and Hg into Au_{25} nanocluster *via* using Au_{25} nanocluster as template, as a result, a series of alloy nanoclusters $Cu_xAu_{25-x}(SR)_{18}$, $Ag_xAu_{25-x}(SR)_{18}$, $Cd_1Au_{24}(SR)_{18}$ and $Hg_1Au_{24}(SR)_{18}$ were obtained [37,38]. Nair *et al.* reported that Pd atom could replace the central atom of Au_{13} icosahedrons in $[Au_{24}Pd(PPh_3)_{10}(SC_2H_4Ph)_5Cl_2]^+$, which led to the dipole moment and excellent stability [39]. Meanwhile, Tlahuice-Flores *et al.* [40] carried out TD-DFT calculation to study a series of Ag doped Au_{18} nanoclusters. And it was found that $Au_{18-x}Ag_x$ nanocluster shows enhanced oscillator strength of HOMO-LOMO due to Ag doping. In addition, $Au_{18-x}Ag_x$ nanocluster exhibited different optical properties and Circular Dichroism in comparison with Au_{18} nanocluster. Wang *et al.* [22] reported Ag atoms substituted Au_{25} nanocluster displaying a 200-fold photoluminescence quantum yield than parent Au_{25} nanocluster. DFT theory indicated that Ag atom in the central site of $Au_{25-x}Ag_x$ nanocluster could stabilize the charges on LUMO orbit and improve its rigidity [41]. Additionally, Ag doped $Au_{23-x}Ag_x$ (x = 4–7) nanocluster was observed to show a distinctly higher catalytic activity than Au_{23} in the photocatalytic degradation of organic pollutants [31]. Unitl now, although many types of foreign atoms have been doped into Au nanoclusters, the synthesis and determination of Au alloy nanoclusters with novel crystal structures are still a huge challenge.

* Corresponding authors.
E-mail addresses: chaoliu@dicp.ac.cn (C. Liu), jiahuihuang@dicp.ac.cn (J. Huang).

https://doi.org/10.1016/j.cclet.2020.02.041
1001-8417/

With respect to metal nanoclusters with the same molecular formula, there are two typical phenomena: structural isomerism and polymorphism. Structural isomerism is observed in gold and silver nanoclusters, which is beneficial to understand the structure-property relationship due to the different properties among isomers [42–44]. In recent work, a few reports focused on the structural isomers because the synthesis and structural determination were difficult. Tian *et al.* [45] reported two Au_{38} isomers and found that Au_{38T} isomer is composed of Au_{25} inner core and exhibited much better catalytic activity in the hydrogenation of 4-nitrophenol. Besides, Pt doping Ag_{29} isomers showed different symmetries and optical properties [46]. In term of polymorphism, atomic packing mode are almost the same apart from different bond lengths and bond angles. However, there are few reports on polymorphism in gold, silver and alloy nanoclusters [47].

Previously, Jin *et al.* synthesized $Au_{19}Ag_4(S\text{-}Adm)_{15}$ nanocluster with $P2_1/n$ space group in tetrahydrofuran (named as NC-$P2_1/n$) [25]. We changed reaction solvent and molar ratio of metal precursors to obtain two polymorphic $Au_{19}Ag_4(S\text{-}Adm)_{15}$ nanoclusters. It is the first time to observe polymorphism in AuAg alloy nanoclusters. In this work, two polymorphs of $Au_{19}Ag_4(S\text{-}Adm)_{15}$ were determined by X-ray crystallography. And they adoped P-1 and $P2_1/c$ space group (named as NC-P-1 and NC-$P2_1/c$, respectively). The optical properties of the $Au_{19}Ag_4(S\text{-}Adm)_{15}$ polymorphs were analyzed by ultra-visible (UV–vis) absorption and fluorescence.

NC-P-1 was synthesized by a simple wet chemical method: $HAuCl_4{\cdot}4H_2O$ (40.9 mg, 0.099 mmol) was dissolved in 5 mL H_2O and 10 mL dichloromethane in the presence of TOAB (63.0 mg, 0.115 mmol). After reaction for 30 min, the aqueous phase in the upper layer was removed. $AgNO_3$ (2.5 mg, 0.015 mmol, molar ratio of Au:Ag = 1:0.15) was dissolved in 1 mL methanol and then poured into above solution. Subsequently, HS-Adm (83.4 mg, 0.496 mmol) was added as thiol. After stirring for 1 h, $NaBH_4$ (37.6 mg, 0.994 mmol, dissolved in 5 mL cold water) was used to reduce the M-SR (M: Au, Ag) polymer. After stirring for four days, the reaction was stopped and the solution was dried with vacuum rotary evaporator. The crude product was washed with methanol for four times and extracted by acetone. Finally, the product was collected by evaporating acetone under vacuum condition. The final dark red crystals were obtained by a vapor diffusion of methanol to toluene at room temperature. The yield of NC-P-1 was ~11% (based on $HAuCl_4$). Synthesis of NC-$P2_1/c$ was followed by the synthetic process of NC-P-1, except for the molar ratio of metal precursors molar ratio of (Au:Ag = 1:0.125). The crude product was washed with methanol for several times and extracted by acetone. To obtain the pure NC-$P2_1/c$ nanocluster, the crude product was kept in the solvent of methanol and toluene (1:1, v:v) for a week. The NC-$P2_1/c$ was dissolved in the mixture solvent of methanol and toluene. At last, the pure NC-$P2_1/c$ was obtained by evaporating the solvent of methanol and toluene. The final crystals were grown up by diffusing methanol to toluene at room temperature. The yield of NC-$P2_1/c$ was ~18% (based on $HAuCl_4$). Crystallographic data of NC-P-1 and NC-$P2_1/c$ is submitted to the Cambridge Crystallographic Data Centre under Nos. 1954872 and 1954873 respectively.

The NC-P-1 nanocluster adopts P-1 space group and it has an icosahedral $Au_{10}Ag_3$ kernel (Fig. 1a). The details of crystallographic data were seen in Table S1 (Supporting information). In this nanocluster, three silver atoms doping in the M_{13} kernel form a triangle on the top of the icosahedron. The other doping silver atom binds with three sulfur atoms to form a AgS_3 motif at the bottom of nanocluster. The kernel is capped by three trimeric $Au_3(SR)_4$ motifs and a AgS_3 motif. There is no silver atom doping into the $Au_3(SR)_4$ motifs (Fig. 1b). In the structural diagram of NC-P-1 nanocluster, it can be seen that the three Ag atoms forming a triangle locate on the top of kernel, and the simple motif AgS_3 is binding at the bottom of the kernel. The Au-Ag bond length of silver atom in the AgS_3 motif

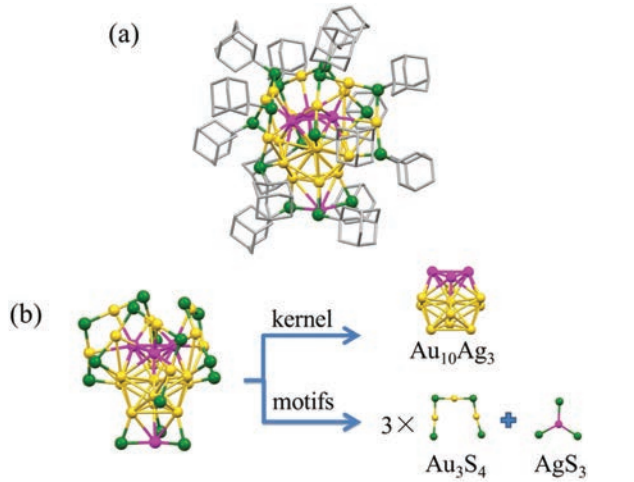

Fig. 1. (a) The total crystal structure of NC-P-1 without hydrogen atoms for clarity. (b) Anatomy of NC-P-1 structure. Color code: yellow, Au; purple, Ag; green, S; grey, C.

and the neighboring three gold atoms is 2.96 Å, 2.97 Å and 3.01 Å respectively. NC-$P2_1/c$ is composed of the same kernel and motifs. The detailed crystallographic data of NC-$P2_1/c$ nanocluster was shown in Fig. S1 and Table S2 (Supporting information).

The molecular structures of NC-P-1 and NC-$P2_1/c$ are similar to that of the previously reported NC-$P2_1/n$ [25]. To further explain the relationship of three nanoclusters, we distinguished the difference of synthetic method and structures. The reported NC-$P2_1/n$ was synthesized in tetrahydrofuran with 1:0.125 molar ratio of gold to silver precursors (Fig. 2a) [25]. NC-$P2_1/c$ was obtained when we changed the reaction solvent from tetrahydrofuran to dichloromethane (Fig. 2b). Based on synthetic method of NC-$P2_1/n$, NC-P-1 was synthesized *via* modulating molar ratio of gold to silver precursors from 1:0.125 to 1:0.15 (Fig. 2c). Crystallographic data of three polymorphs were displayed in Fig. 2d. The crystal system of NC-P-1 is triclinic with the space group P-1. However, NC-$P2_1/c$ and NC-$P2_1/n$ were packed in monoclinic lattice with $P2_1/c$ and $P2_1/n$ space group respectively. In details, unit cell parameters of NC-P-1 are: $a = 17.831(4)$ Å, $b = 20.925(4)$ Å, $c = 29.277(6)$ Å, $\alpha = 83.33(3)^\circ$, $\beta = 81.97(3)^\circ$, $\gamma = 68.35(3)^\circ$. Unit cell parameters of NC-$P2_1/c$ are: $a = 17.1868(2)$ Å, $b = 21.2527(2)$ Å, $c = 58.8533(7)$ Å, $\alpha = 90^\circ$, $\beta = 93.378(1)^\circ$, $\gamma = 90^\circ$ and the unit cell parameters of NC-$P2_1/n$ are: $a = 17.4011(6)$ Å, $b = 44.214(2)$ Å, $c = 30.3350(13)$ Å, $\alpha = 90^\circ$, $\beta = 93.106(3)^\circ$, $\gamma = 90^\circ$. The number of molecules per unit cell (Z), volume and density of the three polymorphs are also showed in Fig. 2d, indicating the distinct difference among these unit cell parameters.

To further understand the difference of the three polymorphs, typical bond lengths of NC-P-1, NC-$P2_1/c$ and NC-$P2_1/n$ were compared (Fig. S2 in Supporting information). The average Au-Ag bond length in the $Au_{10}Ag_3$ kernel of NC-$P2_1/c$ is 2.903 Å, shorter than that of NC-P-1 (2.913 Å) and NC-$P2_1/n$ (2.915 Å). In term of the average Ag-Ag bond length in the kernel, that of NC-P-1 is the shortest (2.868 Å) compared to NC-$P2_1/n$ (2.888 Å) and NC-$P2_1/c$ (2.931 Å). However, the average Au-Au bond length in the kernel of NC-$P2_1/n$ is longer (2.8547 Å) than that of NC-$P2_1/c$ (2.8461 Å) and NC-P-1 (2.8462 Å). In addition, in NC-P-1 nanocluster, the average Ag-Au bond length from kernel to Au_3S_4 motif is 2.988 Å, which is shorter than that in NC-$P2_1/c$ (2.993 Å) and NC-$P2_1/n$ (3.027 Å). However, the average Au-Au bond length from kernel to Au_3S_4 motif of NC-$P2_1/c$ is 3.097 Å, shorter than that of NC-P-1(3.098 Å) and NC-$P2_1/n$ (3.132 Å). More details of the differences in bond lengths of NC-P-1, NC-$P2_1/c$ and NC-$P2_1/n$ are showed in Tables S3-S5 (Supporting information).

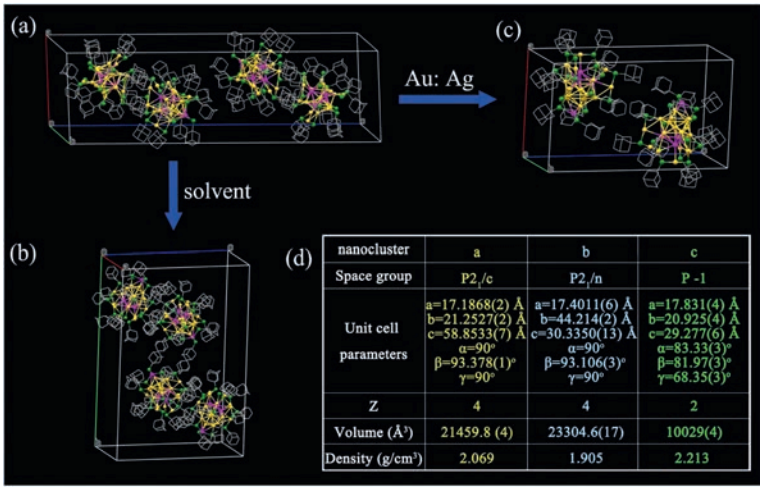

nanocluster	a	b	c
Space group	$P2_1/c$	$P2_1/n$	P -1
Unit cell parameters	a=17.1868(2) Å b=21.2527(2) Å c=58.8533(7) Å α=90° β=93.378(1)° γ=90°	a=17.4011(6) Å b=44.214(2) Å c=30.3350(13) Å α=90° β=93.106(3)° γ=90°	a=17.831(4) Å b=20.925(4) Å c=29.277(6) Å α=83.33(3)° β=81.97(3)° γ=68.35(3)°
Z	4	4	2
Volume (Å^3)	21459.8 (4)	23304.6(17)	10029(4)
Density (g/cm^3)	2.069	1.905	2.213

Fig. 2. Unit cell of (a) NC-$P2_1/n$; (b) NC-$P2_1/c$; (c) NC-P-1. (d) Table of parameters of the three polymorphs. Color code: yellow, Au; purple, Ag; green, S; grey, C.

In addition, these polymorphs show different bond angles. The three bond angles (∠S-Ag-S) in AgS_3 motif of NC-P-1 are 118.37°, 119.54° and 120.72° respectively, indicating the atoms of AgS_3 motif are not in the same plane (Fig. S3 in Supporting information). The average bond angle (∠S-Ag-S) in AgS_3 motif of NC-P-1 is 119.54°, which is larger than that of NC-$P2_1/c$ (119.22°) and NC-$P2_1/n$ (119.18°). The average bond angle (∠Au-S-Au) in Au_3S_4 motif (Fig. S4a in Supporting information) of NC-P-1 (94.51°) is also larger than that of NC-$P2_1/c$ (94.08°) and NC-$P2_1/n$ (93.61°). In Fig. S4b (Supporting information), for the M_{13} core, the average bond angle (∠Ag-Au_c-Au) of NC-P-1, NC-$P2_1/c$ and NC-$P2_1/n$ are 134.67°, 134.66° and 134.63°, showing the slight difference among NC-P-1, NC-$P2_1/c$ and NC-$P2_1/n$. More details of the bond lengths and bond angles of NC-P-1, NC-$P2_1/c$ and NC-$P2_1/n$ were showed in Tables S6-S11 (Supporting information). Of note, it was the first time to find the polymorphs in AuAg alloy nanoclusters.

Many factors influence the synthesis of alloy nanoclusters, such as solvent, molar ratio of metal precursors. It is important to explore the influence factors on the formation of polymorphs. Firstly, we investigated the effect of solvents on the polymorphs. When the dichloromethane was used as solvent instead of tetrahydrofuran, the NC-$P2_1/c$ with $P2_1/c$ space group was obtained. In previous work, reaction solvent has important effect on the size of gold nanoclusters [48]. In our case, it also indicated reaction solvent may lead to the formation of polymorphs. Recently, Jin *et al.* [25] reported a series of AuAg alloy nanoclusters *via* changing the molar ratio of $HAuCl_4$ to $AgNO_3$ precursors. Therefore, we further studied the effect of the molar ratio of Ag to Au on polymorphs. Interestingly, the tuning of molar ratio of $AgNO_3$ to $HAuCl_4$ gives rise to the polymorphs of NC-P-1 in dichloromethane solvent. This demonstrated that molar ratio of metal precursors plays an important role in preparing polymorphs of Au-Ag alloy nanoclusters.

The optical properties of metal nanoclusters are sensitive to the structures. To investigate optical properties of the polymorphs, we carried out UV–vis spectrometry and fluorescence. In Fig. 3a, the NC-P-1 shows the prominent absorption peaks at 730 nm, 580 nm, 460 nm and 440 nm. All the absorption peaks of NC-P-1 display the obvious blue shift by 20 nm than those of NC-$P2_1/n$ [25]. However, NC-$P2_1/c$ shows UV–vis absorption peaks at 490 nm and 580 nm with a shoulder at 380 nm. It further indicates that the three polymorphs exhibit different optical properties, which may result of their structures.

To further test the difference of optical properties, we studied the fluorescence of the three polymorphs. Fig. 3b demonstrated

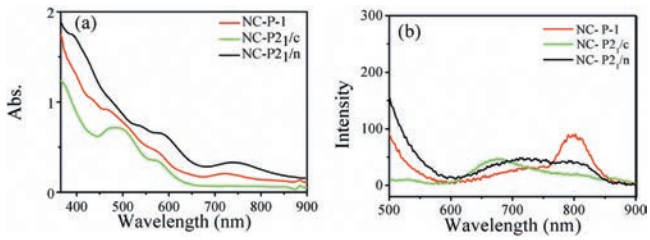

Fig. 3. (a) UV–vis absorption spectrum of NC-P-1, NC-$P2_1/c$ and NC-$P2_1/n$ [25] and (b) Fluorescence spectra of the NC-P-1, NC-$P2_1/c$ and NC-$P2_1/n$ (dissolved in dichloromethane).

that NC-$P2_1/n$ exhibits a weak emission at 800 nm and 720 nm. NC-$P2_1/c$ only shows a peak at 680 nm. However, the NC-P-1 exhibits the enhanced fluorescence at 800 nm. By comparison, it was found that the fluorescence of NC-P-1 is almost close to near infrared range. It can be inferred that the structures of Au-Ag alloy nanoclusters have a significant effect on the optical properties.

The thermal stability of nanocluster is related to their structures [49,50]. To study the thermal stability of the three polymorphs, the samples were heated at different temperatures. The NC-P-1 nanocluster showed pretty well stability at 60 °C. After heating at 60 °C for 18 h, the absorption peaks intensity was kept very well, similar to those before heating. When heating at 60 °C for 50 h, the absorption peaks became weak. The peak at 750 nm disappeared after reaction for 72 h, which means that the NC-P-1 nanocluster collapsed (Fig. 4a). The stability of NC-P-1 was also tested at 80 °C.

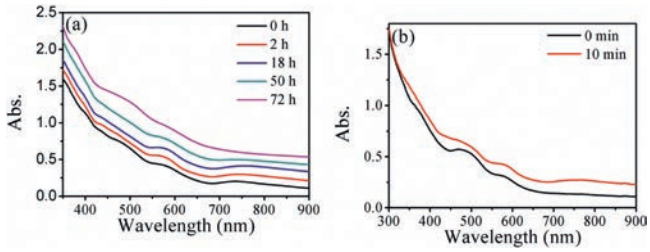

Fig. 4. Thermal stability test of (a) NC-P-1 and (b) NC-$P2_1/c$ nanoclusters at 60 °C in toluene.

It showed the NC-P-1 could keep stable at 80 °C for 22 h. However, after reaction for 39 h, the UV–vis spectrum shows there is no prominent absorption peak (Fig. S5 in Supporting information). We also carried out the heat treatment of the NC-$P2_1/c$. When heating at 60 °C for 10 min, the peaks at 760 nm rapidly faded away (Fig. 4b). Even at room temperature, NC-$P2_1/c$ only kept stable for 1 h in toluene (Fig. S6 in Supporting information). Thermal stability of NC-$P2_1/n$ was also tested at 80 °C and it broke down after 2 h [25]. On the basis of the experimental data, it is clear that NC-P-1 possesses much better thermal stability than NC-$P2_1/c$ and NC-$P2_1/n$, and this clear difference in thermal stability should be caused by their different structures.

In summary, we synthesized two polymorphs of $Au_{19}Ag_4(S\text{-}Adm)_{15}$ nanoclusters *via* changing the reaction solvent and molar ratio of $AgNO_3$ to $HAuCl_4$. In our work, it was found that solvent and molar ration of metal precursor have great effect on the synthesis of polymorphs. The two Au-Ag nanoclusters adopt P-1 and $P2_1/c$ space group respectively. The structures of Au-Ag alloy nanoclusters were determined by X-ray crystallography, which is composed of an icosahedral $Au_{10}Ag_3$ kernel, three Au_3S_4 motifs and a AgS_3 motif. The three polymorphs showed different optical properties and thermal stability. NC-P-1 showed the enhanced fluorescence and exhibited well thermal stability. It can keep stable even heating at high temperature of 80 °C for 22 h. This study opens a new way for exploring chemical and physical properties of polymorphs in metal nanoclusters and providing the insight into understanding their structure-property relationship in the future.

Declaration of competing interest

The authors declare that they have no known competing financial interests or personal relationships that could have appeared to influence the work reported in this paper.

Acknowledgments

We acknowledge the National Natural Science Foundation of China (No. 21601178). We sincerely thank Yingwei Li and Rongchao Jin from Department of Chemistry, Carnegie Mellon University. We thank staffs at the Shanghai Synchrotron Radiation Facility for assistance during the crystallographic data collection.

Appendix A. Supplementary data

Supplementary material related to this article can be found, in the online version, at doi:https://doi.org/10.1016/j.cclet.2020.02.041.

References

[1] Q. Yu, P.L. Gao, K.Y. Zhang, et al., Light-Sci Appl. 6 (2017) e17107.
[2] D.H. Tian, Z.S. Qian, Y.S. Xia, C.Q. Zhu, Langmuir 28 (2012) 3945–3951.
[3] K. Saha, S.S. Agasti, C. Kim, X.N. Li, V.M. Rotello, Chem. Rev. 112 (2012) 2739–2779.
[4] X. Yang, M.X. Yang, B. Pang, M. Vara, Y.N. Xia, Chem. Rev. 115 (2015) 10410–10488.
[5] Z.T. Luo, K.Y. Zheng, J.P. Xie, Chem. Commun. 50 (2014) 5143–5155.
[6] J. Xu, L. Shang, Chin. Chem. Lett. 29 (2018) 1436–1444.
[7] H.D. Cui, D.H. Hu, J.N. Zhang, et al., Chin. Chem. Lett. 28 (2017) 1391–1398.
[8] Z. Wu, D.R. Mullins, L.F. Allard, Q. Zhang, L. Wang, Chin. Chem. Lett. 29 (2018) 795–799.
[9] Y. Tan, X.Y. Liu, L. Li, et al., J. Catal. 364 (2018) 174–182.
[10] G. Li, H. Abroshan, C. Liu, et al., ACS Nano 10 (2016) 7998–8005.
[11] B. Yoon, H. Hakkinen, U. Landman, et al., Science 307 (2005) 403–407.
[12] H. Zhu, N. Goswami, Q. Yao, et al., J. Mater. Chem. A 6 (2018) 1102–1108.
[13] F. Xu, J. Chen, S. Kalytchuk, et al., J. Catal. 354 (2017) 1–12.
[14] X. Yuan, Z.T. Luo, Y. Yu, Q.F. Yao, J.P. Xie, Chem. Asian J. 8 (2013) 858–871.
[15] H.F. Qian, D.E. Jiang, G. Li, et al., J. Am. Chem. Soc. 134 (2012) 16159–16162.
[16] Y. Niihori, W. Kurashige, M. Matsuzaki, Y. Negishi, Nanoscale 5 (2013) 508–512.
[17] T. Chen, S. Yang, J. Chai, et al., Sci. Adv. 3 (2017) e1700956.
[18] M.A. Tofanelli, T.W. Ni, B.D. Phillips, C.J. Ackerson, Inorg. Chem. 55 (2016) 999–1001.
[19] G. Soldan, M.A. Aljuhani, M.S. Bootharaju, et al., Angew. Chem. Int. Ed. 55 (2016) 5749–5753.
[20] Y.B. Song, S. Jin, X. Kang, et al., Chem. Mater. 28 (2016) 2609–2617.
[21] T. Cesca, B. Kalinic, N. Michieli, et al., Phys. Chem. Chem. Phys. 17 (2015) 28262–28269.
[22] S. Wang, X. Meng, A. Das, et al., Angew. Chem. Int. Ed. 53 (2014) 2376–2380.
[23] Y. Negishi, M. Mizuno, M. Hirayama, et al., Nanoscale 5 (2013) 7188–7192.
[24] C.A. Fields-Zinna, M.C. Crowe, A. Dass, J.E.F. Weaver, R.W. Murray, Langmuir 25 (2009) 7704–7710.
[25] Y. Li, T.Y. Luo, M. Zhou, et al., J. Am. Chem. Soc. 140 (2018) 14235–14243.
[26] X. Kang, L. Xiong, S. Wang, Y. Pei, M. Zhu, Inorg. Chem. 57 (2018) 335–342.
[27] C. Kumara, C.M. Aikens, A. Dass, J. Phys, Chem. Lett. 5 (2014) 461–466.
[28] V.R. Jupally, A. Dass, Phys. Chem. Chem. Phys. 16 (2014) 10473–10479.
[29] C. Kumara, A. Dass, Nanoscale 4 (2012) 4084–4086.
[30] S. Malola, H. Hakkinen, J. Phys. Chem. Lett. 2 (2011) 2316–2321.
[31] C. Liu, X.Q. Ren, F. Lin, et al., Angew. Chem. Int. Ed. 58 (2019) 11335–11339.
[32] X. Kang, M. Zhou, S. Wang, et al., Chem. Sci. 8 (2017) 2581–2587.
[33] S. Tian, L. Liao, J. Yuan, et al., Chem. Commun. 52 (2016) 9873–9876.
[34] S. Wang, Y. Song, S. Jin, et al., J. Am. Chem. Soc. 137 (2015) 4018–4021.
[35] E. Gottlieb, H.F. Qian, R.C. Jin, Chem: Eur J. 19 (2013) 4238–4243.
[36] Y. Negishi, K. Munakata, W. Ohgake, K. Nobusada, J. Phys, Chem. Lett. 3 (2012) 2209–2214.
[37] C. Yao, Yj. Lin, J. Yuan, et al., J. Am. Chem. Soc. 137 (2015) 15350–15353.
[38] L.W. Liao, S.M. Zhou, Y.F. Dai, et al., J. Am. Chem. Soc. 137 (2015) 9511–9514.
[39] L.V. Nair, S. Hossain, S. Takagi, et al., Nanoscale 10 (2018) 18969–18979.
[40] B. Molina, A. Tlahuice-Flores, Phys. Chem. Chem. Phys. 18 (2016) 1397–1403.
[41] M. Zhou, J. Zhong, S. Wang, et al., J. Phys. Chem. C 119 (2015) 18790–18797.
[42] L.Q. Wang, X.Q. Chai, X.L. Cheng, Y. Zhu, ChemistrySelect 3 (2018) 6165–6169.
[43] M. Zhou, S.B. Tian, C.J. Zeng, et al., J. Phys. Chem. C 121 (2017) 10686–10693.
[44] R. Juarez-Mosqueda, S. Malola, H. Hakkinen, Eur. Phys. J. D 73 (2019) 62–68.
[45] S. Tian, Y.Z. Li, M.B. Li, et al., Nat. Commun. 6 (2015) 8667.
[46] X. Lin, C. Liu, K. Sun, et al., Nano Res. 12 (2019) 309–314.
[47] A. Nag, P. Chakraborty, M. Bodiuzzaman, et al., Nanoscale 10 (2018) 9851–9855.
[48] C. Liu, G. Li, G. Pang, R. Jin, RSC Adv. 3 (2013) 9778–9784.
[49] X. Kang, C. Silalai, Y. Lv, et al., Eur. J. Inorg. Chem. 2017 (2017) 1414–1419.
[50] Q. Tang, R.H. Ouyang, Z.Q. Tian, D.E. Jiang, Nanoscale 7 (2015) 2225–2229.